DOI: 10.1021/om1000327

ORGANOMETALLICS
Article

Synthesis, Structure, and Temperature-Dependent Dynamics of Neutral Palladium Allyl Complexes of Annulated Diaminocarbenes and Their Catalytic Application for C−C and C−N Bond Formation Reactions†

Sarim Dastgir,*[,‡,§] Karl S. Coleman,[⊥] Andrew R. Cowley,[‡] and Malcolm L. H. Green*[,‡]

[‡]*Inorganic Chemistry Laboratory, University of Oxford, South Parks Road, Oxford, OX1 3QR, U.K., and* [⊥]*Department of Chemistry, Durham University, South Road, Durham, DH1 3LE, U.K.* [§]*Present address: Department of Chemistry, York University, 4700 Keele St., Toronto, ON, M3J 2Z3, Canada. Tel: +1 416 736 2100, ext. 77720. Fax: +1 416 736 5936*

Received January 11, 2010

Imidazolinium salts 7,9-bis(2,4,6-trimethylphenyl)-6b,9a-dihydroacenaphtho[1,2-*d*]imidazolinium tetrafluoroborate and 7,9-bis(2,6-diisopropylphenyl)-6b,9a-dihydroacenaphtho[1,2-*d*]imidazolinium tetrafluoroborate, designated as [(BIAN-SIMes)(H)]BF_4 (**3a**) and [(BIAN-SIPr)(H)]BF_4 (**3b**), respectively, have been prepared and structurally characterized. The molecular structure of **3a** shows the presence of a bifurcated hydrogen bond between the tetrafluoroborate anions and the central imidazolinium proton (−NC*H*N−). The palladium(II) complexes (η^3-C_3H_5)Pd(BIAN-SIMes)Cl (**5a**) and (η^3-C_3H_5)Pd(BIAN-SIPr)Cl (**5b**) have been synthesized. The temperature-dependent NMR behavior of σ-bonded palladium(II) complex **5b** was studied. The crystal structure of **5b** shows a localized single and double bond between the allyl ligand. The catalytic activities of the palladium(II) complexes **5a** and **5b** have been evaluated for Suzuki-type C−C coupling and for room-temperature C−N bond formation using aryl halides.

Introduction

Almost two decades after the pioneering work by Wanzlick et al.,[1] Öfele et al.,[2] and Lappert et al.[3] on the coordination chemistry of N-heterocyclic carbenes (NHCs), the first stable imidazole-2-ylidene (NHC) was isolated in 1991 by Arduengo et al.[4,5] Since then, the chemistry of these potent σ-donors species (NHCs) have sparked renewed interest in the coordination chemistry of such ligands as an alternative to more ubiquitous tertiary phosphines due to their similarities in terms of thermodynamics and coordination behavior;[6−9] however, the degree of π-back-bonding in NHCs has been discussed extensively in recent literature.[10−14] The strong σ-donating ability of the NHC ligands results in the formation of stable metal−NHC bonds, which are less prone to reductive elimination and to degradative cleavage during catalytic reactions;[12,13,15] however, their reductive elimination pathways have also been studied in detail.[16] Recently, large numbers of NHC complexes have shown potential as catalysts for a wide range of organic transformations, including metathesis[17,18] and cross-coupling reactions.[19−22] Unlike phosphines,[23] the steric and electronic tunability of

† Part of the Dietmar Seyferth Festschrift.

*Corresponding authors. Tel: +44 (0) 1865 272600. Fax: +44 (0) 1865 272690. E-mail: malcolm.green@chem.ox.ac.uk; sarim.dastgir@lmh.oxon.org.

(1) Wanzlick, H. W.; Schoenherr, H. J. *Angew. Chem., Int. Ed. Engl.* **1968**, *7*, 141–142.
(2) Öfele, K.; Herberhold, M. *Angew. Chem., Int. Ed. Engl.* **1970**, *9*, 739–740.
(3) Cardin, D. J.; Çetinkaya, B.; Lappert, M. F.; Manojlović-Muir, L.; Muir, K. W. *J. Chem. Soc. D, Chem. Commun.* **1971**, 400–401.
(4) Arduengo, A. J. *Acc. Chem. Res.* **1999**, *32*, 913–921.
(5) Arduengo, A. J.; Harlow, R. L.; Kline, M. *J. Am. Chem. Soc.* **1991**, *113*, 361–363.
(6) Gibson, S. E.; Johnstone, C.; Loch, J. A.; Steed, J. W.; Stevenazzi, A. *Organometallics* **2003**, *22*, 5374–5377.
(7) Duan, W.-L.; Shi, M.; Rong, G.-B. *Chem. Commun.* **2003**, *23*, 2916–2917.
(8) Douthwaite, R. E.; Hauessinger, D.; Green, M. L. H.; Silcock, P. J.; Gomes, P. T.; Martins, A. M.; Danopoulos, A. A. *Organometallics* **1999**, *18*, 4584–4590.
(9) Douthwaite, R. E.; Green, M. L. H.; Silcock, P. J.; Gomes, P. T. *J. Chem. Soc., Dalton Trans.* **2002**, 1386–1390.
(10) Bourissou, D.; Guerret, O.; Gabbaï, F. P.; Bertrand, G. *Chem. Rev.* **2000**, *100*, 39–92.
(11) Herrmann, W. A.; Köcher, C. *Angew. Chem., Int. Ed. Engl.* **1997**, *36*, 2162–2187.
(12) Herrmann, W. A. *Angew. Chem., Int. Ed.* **2002**, *41*, 1290–1309.
(13) Crabtree, R. H. *J. Organomet. Chem.* **2005**, *690*, 5451–5457.
(14) Khramov, D. M.; Lynch, V. M.; Bielawski, C. W. *Organometallics* **2007**, *26*, 6042–6049.
(15) Glorius, F., Ed. *N-Heterocyclic Carbenes in Transition Metal Catalysis*; Topics in Organometallic Chemistry, Vol. 21; Springer-Verlag: Berlin/Heidelberg, 2007.
(16) Cavell, K. *Dalton Trans.* **2008**, 6676–6685, and references therein..
(17) Connon, S. J.; Blechert, S. *Angew. Chem., Int. Ed.* **2003**, *42*, 1900–1923.
(18) Trnka, T. M.; Grubbs, R. H. *Acc. Chem. Res.* **2000**, *34*, 18–29.
(19) Grasa, G. A.; Viciu, M. S.; Huang, J.; Zhang, C.; Trudell, M. L.; Nolan, S. P. *Organometallics* **2002**, *21*, 2866–2873.
(20) Navarro, O.; Kaur, H.; Mahjoor, P.; Nolan, S. P. *J. Org. Chem.* **2004**, *69*, 3173–3180.
(21) Hartwig, J. F. *Acc. Chem. Res.* **2008**, *41*, 1534–1544.
(22) Kotha, S.; Lahiri, K.; Kashinath, D. *Tetrahedron* **2002**, *58*, 9633–9695.
(23) McAuliffe, C. A. Phosphorous, Arsenic, Antimony and Bismuth Ligands. In *Comprehensive Coordination Chemistry*; Wilkinson, G.; Gillard, R. D.; McCleverty, J. A., Eds.; Pergamon Press: Oxford, 1987; Vol. 2, pp 989−1066.

 Published on Web 05/13/2010

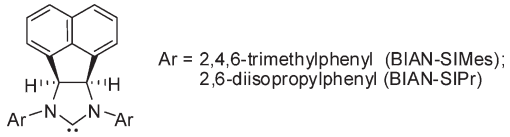

Figure 1. Stable acenaphthylene-annulated diamino carbene ligands.

Scheme 1. Synthesis of Imidazolium Salts

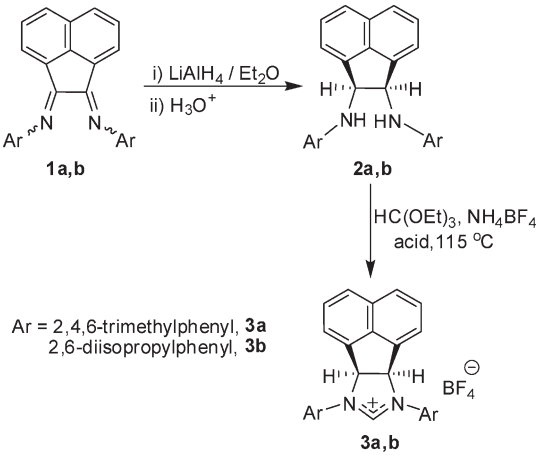

NHCs is more restricted due to their confined architectures. Studies on the annulated backbone (C_4-C_5)-substituted NHCs have demonstrated that the stability[24−29] and the σ-donating ability of NHCs vary substantially with a change in the substituent (π-donor/acceptor) attached to the imidazole ring and may be used as a tool for the fine-tuning of the electronic properties.[30−32] A range of annulated NHC complexes have been synthesized by *in situ* trapping of the carbene with suitable metal precursors, but the corresponding NHCs were not isolated, presumably due to the more ubiquitous dimerization of saturated carbenes to produce enetetramines.[24,26−28]

Scheme 2. Synthesis of (η^3-C_3H_5)Pd(BIAN-SIAr)Cl Complexes[a]

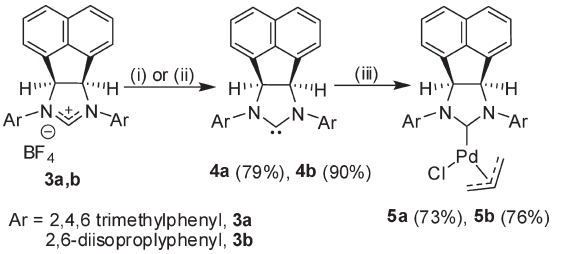

[a] (i) KO^{t}Bu/THF, −78 °C (**3a**); (ii) ^{n}BuLi/pentane, −78 °C (**3b**); (iii) [(η^3-C_3H_5)Pd(μ-Cl)]$_2$/THF, −78 °C (10 min) to room temperature (3 h).

In our studies of the organometallic chemistry of NHCs,[8,33−38] we have recently described the first stable acenaphthylene-annulated backbone (C_4-C_5) diamino carbene ligand[39] (Figure 1) and its coordination with rhodium(I) and iridium(I). The presence of substantial steric bulk located away from the coordination site could modify the coordination behavior of these ligands and thereby provide the opportunity for catalyst fine-tuning. Here we report the synthesis of ligand precursors [(BIAN-SIMes)(H)]BF_4 (**3a**) and [(BIAN-SIPr)(H)]BF_4 (**3b**) (Scheme 1) and their coordination to palladium using [Pd(η^3-C_3H_5)(μ-Cl)]$_2$, Scheme 2. The variable-temperature dynamics for the corresponding palladium allyl complexes and their catalytic behavior for Suzuki-type C−C coupling and room-temperature C−N bond formation using aryl halides have also been investigated.

Results and Discussion

Synthesis and Characterization of the Imidazolinium Salts [(BIAN-SIMes)(H)]BF_4 (3a) and [(BIAN-SIPr)(H)]BF_4 (3b). Our investigation of the synthesis of imidazolinium salts [(BIAN-SIMes)(H)]BF_4 (**3a**) and [(BIAN-SIPr)(H)]BF_4 (**3b**) started with the synthesis of bis(aryl)acenaphthenequinonediimine **Ar-BIAN**, where Ar = 2,4,6-trimethylphenyl (**1a**)[40] and 2,6-diisopropylphenyl (**1b**).[41] The reduction of **Ar-BIAN** with $LiAlH_4$ produced (1*R*,2S)-*N,N*-bis(aryl)-1,2-dihydroacenaphthylene-1,2-diamine, which on cyclization with triethyl orthoformate in the presence NH_4BF_4 and an acid catalyst gave the imidazolinium salts **3a** and **3b** as off-white solids in good yields (60−75%), Scheme 1. The imidazolinium salts **3a** and **3b** were characterized by elemental analysis, mass spectrometry (ES^+), single-crystal X-ray diffraction analysis, and ^1H and ^{13}C NMR studies using gCOSY, HMBC, HMQC, DEPT, and TOCSY experiments.

As expected, the ^1H NMR ($CDCl_3$) spectrum of imidazolinium salt **3a** shows the presence of one set of three characteristic resonances for the mesityl CH_3 protons at δ 2.60, 2.34, and 1.42, while the mesityl *m*-CH protons appeared as a set of two broad singlets at δ 7.09 and 6.87, respectively. On the other hand, the ^1H NMR ($CDCl_3$) spectrum of imidazolinium salt **3b** showed a typical AX_2 spectrum as two sets of four doublets for the isopropyl CH_3 protons at δ 1.55 (^3J = 6.6 Hz), 1.34 (^3J = 6.6 Hz), 0.89 (^3J = 6.7 Hz), and 0.72 (^3J = 6.6 Hz), respectively, whereas the isopropyl methine protons were observed as a set of two septets at δ

(24) Hahn, F. E. *Angew. Chem., Int. Ed.* **2006**, *45*, 1348–1352.
(25) Hahn, F. E.; Wittenbecher, L.; Le Van, D.; Frohlich, R. *Angew. Chem., Int. Ed.* **2000**, *39*, 541–544.
(26) Herrmann, W. A.; Baskakov, D.; Herdtweck, E.; Hoffmann, S. D.; Bunlaksananusorn, T.; Rampf, F.; Rodefeld, L. *Organometallics* **2006**, *25*, 2449–2456.
(27) Metallinos, C.; Barrett, F. B.; Chaytor, J. L.; Heska, M. E. A. *Org. Lett.* **2004**, *6*, 3641–3644.
(28) Saravanakumar, S.; Kindermann, M. K.; Heinicke, J.; Köckerling, M. *Chem. Commun.* **2006**, 640–642.
(29) Pause, L.; Robert, M.; Heinicke, J.; Kuhl, O. *J. Chem. Soc., Perkin Trans. 2* **2001**, 1383–1388.
(30) Tapu, D.; Owens, C.; VanDerveer, D.; Gwaltney, K. *Organometallics* **2009**, *28*, 270–276.
(31) Sanderson, M. D.; Kamplain, J. W.; Bielawski, C. W. *J. Am. Chem. Soc.* **2006**, *128*, 16514–16515.
(32) Khramov, D. M.; Lynch, V. M.; Bielawski, C. W. *Organometallics* **2007**, *26*, 6042–6049.
(33) Coleman, K. S.; Chamberlayne, H. T.; Turberville, S.; Green, M. L. H.; Cowley, A. R. *J. Chem. Soc., Dalton Trans.* **2003**, *14*, 2917–2922.
(34) Coleman, K. S.; Dastgir, S.; Barnett, G.; Alvite, M. J. P.; Cowley, A. R.; Green, M. L. H. *J. Organomet. Chem.* **2005**, *690*, 5591–5596.
(35) Coleman, K. S.; Turberville, S.; Pascu, S. I.; Green, M. L. H. *Tetrahedron Lett.* **2004**, *45*, 8695–8698.
(36) Coleman, K. S.; Turberville, S.; Pascu, S. I.; Green, M. L. H. *J. Organomet. Chem.* **2005**, *690*, 653–658.
(37) Dastgir, S.; Coleman, K. S.; Cowley, A. R.; Green, M. L. H. *Organometallics* **2006**, *25*, 300–306.
(38) Douthwaite, R. E.; Green, M. L. H.; Silcock, P. J.; Gomes, P. T. *Organometallics* **2001**, *20*, 2611–2615.
(39) Dastgir, S.; Coleman, K. S.; Cowley, A. R.; Green, M. L. H. *Dalton Trans.* **2009**, 7203–7214.
(40) El-Ayaan, U.; Murata, F.; El-Derby, S.; Fukuda, Y. *J. Mol. Struct.* **2004**, *692*, 209–216.
(41) Paulovicova, A.; El-Ayaan, U.; Shibayama, K.; Morita, T.; Fukuda, Y. *Eur. J. Inorg. Chem.* **2001**, *10*, 2641–2646.

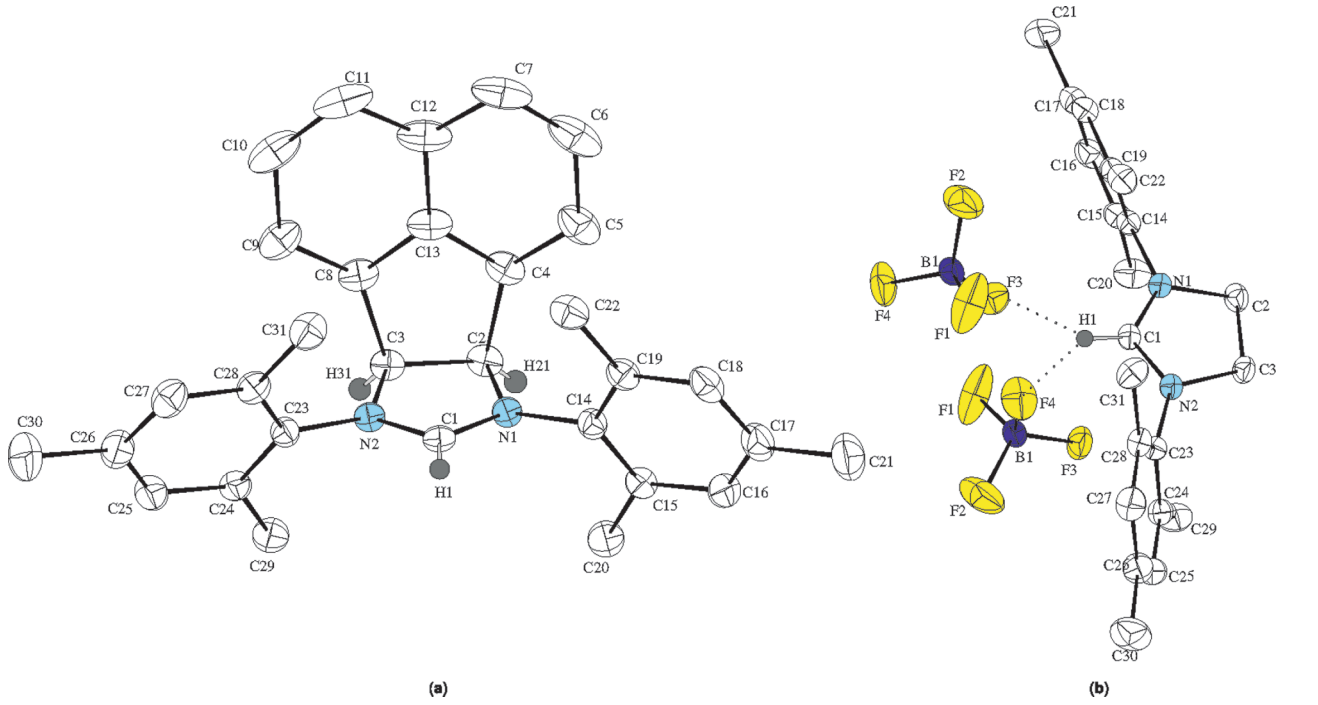

Figure 2. ORTEP diagram of the molecular structure of [(BIAN-SIMes)(H)]BF_4 (**3a**) at 40% probability (a). Solvent molecule and BF_4 anion have been removed for clarity. (b) A bifurcated hydrogen bond between two neighboring BF_4 anions is shown. (Solvent molecules and the backbone naphthyl group have been removed for clarity.)

3.43 (^3J = 6.7 Hz) and 1.94 (^3J = 6.6 Hz), respectively. The *N*-2,6-diisopropylphenyl *m*-CH on either side of the imidazole ring appeared as a set of two doublets of doublets at δ 7.42 (^3J = 7.4 Hz, ^4J = 1.4 Hz) and 7.20 (^3J = 7.6 Hz, ^4J = 1.4 Hz), and the *p*-CH appeared as a triplet at δ 7.48 (^3J = 6.7 Hz). This peak pattern suggests the hindered rotation around the N−aromatic bonds on either side of imidazole rings. The backbone (−NC*H*C*H*N−) protons appear as singlets at δ 6.61 (**3a**) and 6.67 (**3b**), respectively, and the central imidazolinium (−NC*H*N−) proton shows the characteristic downfield resonance at δ 8.19 (**3a**) and 8.18 (**3b**), respectively. In the ^{13}C NMR spectrum the central imidazolinium carbon (−N*C*N−) shows a resonance at δ 157.1 (**3a**) and 156.3 (**3b**), respectively. The (−N*CC*N−) carbons appeared as singlets at δ 70.6 (**3a**) and 72.6 (**3b**), respectively. Full ^{1}H and ^{13}C{^{1}H} assignments for imidazolium salts **3a** and **3b** are detailed in the Experimental Section and are comparable with data reported for similar compounds.[42,43]

Structural Study. To establish the molecular structure for the imidazolinium salts **3a** and **3b**, a single-crystal diffraction analysis was performed on a crystal grown by layering of pentane onto a saturated dichloromethane solution. The ORTEP views of the molecular structures of imidazolinium salts are shown in Figures 2 (**3a**) and 3 (**3b**), and crystal data are summarized in Table 1 in the Supporting Information.

A comparison of the selected bond lengths and angles for imidazolinium salts **3a** and **3b** along with the related structural parameters for 1,3-dimesitylimidazolinium chloride[44]

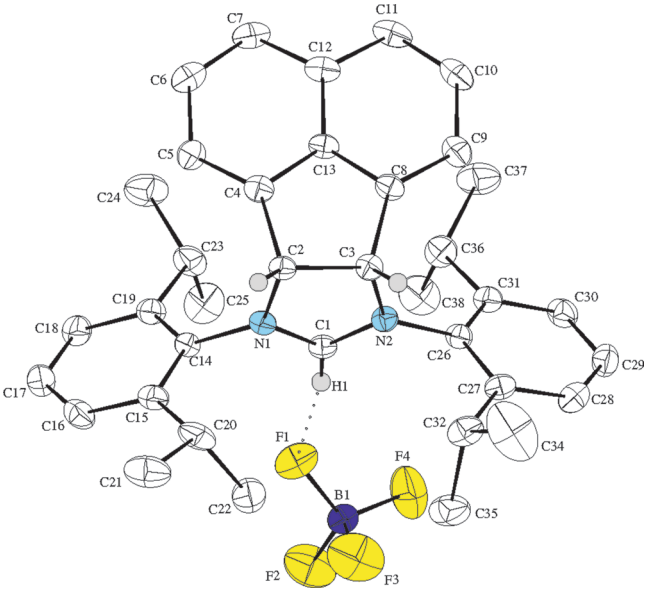

Figure 3. ORTEP diagram of the molecular structure of [(BIAN-SIPr)(H)]BF_4 (**3b**) at 40% probability (solvent molecule has been removed for clarity).

are given in Table 1. The X-ray diffraction analyses for imidazolinium salts **3a** and **3b** reveal that the cations lie on a site with no crystallographic symmetry, but have an approximate local mirror plane. In the molecular structure of imidazolinium salts, the average $C_1-N_{1(2)}$ and $N_{1(2)}-C_{2(3)}$ bond lengths for **3a** and **3b** are on the same order as observed for the [(SIMes)(H)]Cl.[44] Due to ring strain and the presence of the bulky naphthyl group at the backbone, the considerably longer C_2-C_3 bond lengths of 1.560(4) Å, **3a**, and 1.567(3) Å, **3b**, and the $N_{1(2)}-C_{(aromatic)}$ length of 1.442(4) Å,

(42) Arduengo, A. J., III; Krafczyk, R.; Schmutzler, R.; Craig, H. A.; Goerlich, J. R.; Marshall, W. J.; Unverzagt, M. *Tetrahedron* **1999**, *55*, 14523–14534.
(43) Türkmen, H.; Şhin, O.; Büyükgüngör, O.; Çetinkaya, B. *Eur. J. Inorg. Chem.* **2006**, 4915–4921.
(44) Arduengo, A. J., III; Goerlich, J. R.; Marshall, W. J. *J. Am. Chem. Soc.* **1995**, *117*, 11027–11028.

Table 1. Comparison of the Selected Bond Lengths (Å) and Angles (°) for Imidazolinium Salts 3a and 3b with Reported Data

property	[(BIAN-SIMes)(H)]BF_4, **3a**[a]	[(BIAN-SIPr)(H)]BF_4, **3b**[a]	BIAN-SIMes, **4a**[b]	(η^3-C_3H_5)Pd(BIAN-SIPr)Cl, **5b**	[(SIMes)(H)]Cl[c]
			Bond Lengths		
$C_1-N_{1(2)}$	1.315(4), 1.313(4)	1.313(3), 1.317(3)	1.348(2), 1.346(2)	1.344(3), 1.350(3)	1.327(5), 1.310(5)
$N_{1(2)}-C_{2(3)}$	1.496(4), 1.494(4)	1.497(3), 1.490(3)	1.491(2), 1.496(2)	1.484(3), 1.492(3)	1.498(6), 1.487(6)
C_2-C_3	1.560(4)	1.567(3)	1.558(2)	1.555(4)	1.518(7)
$N_{1(2)}-C_{(aromatic)}$	1.442(4), 1.442(4)	1.446(3), 1.440(3)	1.434(2), 1.435(2)	1.447(3), 1.442(3)	1.432(5), 1.437(6)
			Hydrogen Bond Lengths		
H_1-F_3	2.383				
H_1-F_4	2.426				
H_1-F_1		2.198			
			Bond Angles (θ)		
$N_1-C_1-N_2$	113.8(3)	114.0(2)	106.09(14)	108.4(2)	113.1(4)
$C_1-N_{1(2)}-C_{2(3)}$	110.7(2), 110.7(2)	110.5(2), 110.81(19)	115.51(14),115.37(14)	112.9(2),112.9(2)	109.7(4), 110.6(4)
$N_{1(2)}-C_{2(3)}-C_{3(2)}$	102.3(2), 102.5(2)	102.31(18), 102.32(18)	101.51(13),101.43(13)	102.6(2),100.9(2)	103.0(4), 103.3(4)
$C_1-N_{1(2)}-C_{mes}$	126.9(2), 127.9(2)	125.8(2), 126.8(2)	124.01(14), 123.18(14)	129.1(2), 125.8(2)	127.0(4), 126.2(4)
$N_{1(2)}-C_{2(3)}-C_{4(8)}$	113.2(2), 112.5(2)	114.3(2), 113.3(8)	113.97(14), 114.30(14)	117.2(2), 116.2(3)	
			Torsion Angle (θ)		
$N_1-C_2-C_3-N_2$	0.68	2.42	1.97	12.9	

[a] This work. [b] Reference 39. [c] Reference 44.

3a, and 1.443(3) Å, **3b**, were observed. The $N_1-C_1-N_2$ bond angles of 113.8(3)° and 114.0(2)° observed for **3a** and **3b** are on the same order as found for [(SIMes)(H)]Cl,[44] but significantly larger than the corresponding bond angle of 108.7(4)° observed for [(IMes)(H)]Cl.[42] The significantly larger $N_1-C_2-C_4$ and $N_2-C_3-C_8$ bond angles of 114.3(2)° and 113.32(18)° observed for **3b** are due to the greater interaction of the bulky, more hindered isopropyl groups with the naphthyl group attached at the backbone, Table 1. This is further supported by the larger torsion angle of 2.42°, **3b**, when compared with 0.68° observed for **3a**. The angles between the best planes of the dihydroimidazole ring and the naphthyl group are 62.7°, **3a**, and 59.5°, **3b**, respectively. The angle between the best planes of the dihydroimidazole ring and the phenyl rings $C_{15}-C_{14}-C_{19}$ and $C_{24}-C_{23}-C_{28}$ are 78.6° and 72.2°, **3a**, and 79.7° and 80.6°, **3b**, respectively.

It is also noteworthy that the CH group of the imidazolinium ion, **3a**, Figure 2, and two F atoms of the neighboring anion appear to have some interactions: $C_1\cdots F_3$ 3.149(3) Å with symmetry operator $1/2-x$, $1/2+y$, $1/2-z$, $C_1\cdots F_4$ 2.899(3) Å, respectively. Consequently the CH group projects between these F atoms, and this may be considered as a bifurcated hydrogen bond due to the $H_1\cdots F_3$ bond length of 2.383 Å and $H_1\cdots F_4$ bond length of 2.426 Å. In contrast to the imidazolinium salt [(BIAN-H_2IMes)(H)]BF_4, **3a**, the CH group of the imidazole ring in [(BIAN-H_2IPr)(H)]BF_4, **3b**, forms a hydrogen bond only to one of the F atoms of the anion: $H_1\cdots F_1$ bond length of 2.198 Å. The remaining bond lengths and angles are unexceptional and lie within the range expected. Complete details of the single-crystal X-ray analysis are given in the Supporting Information.

Synthesis and Characterization of the Palladium Complexes (η^3-C_3H_5)Pd(BIAN-SIMes)Cl (5a) and (η^3-C_3H_5)Pd(BIAN-SIPr)Cl (5b). The palladium(II) complexes **5a** and **5b** were synthesized by the reaction of the free carbenes with [(η^3-C_3H_5)Pd(μ-Cl)]$_2$ in THF at −78 °C, Scheme 2. After the workup palladium(II) complexes **5a** and **5b** were isolated as air-stable crystalline solids. It is important to mention here that the deprotonation of imidazolinium salts **3a** and **3b** is very much dependent on the choice of an appropriate solvent as well as the base, since a slight change to the imidazolium architecture has a dramatic effect on the clean generation of the corresponding imidazolin-2-ylidene.[39]

NMR Studies. The ^{1}H NMR spectrum for the palladium complex **5a** (room temperature) shows the formation of only one diasteromer, and the assignments were made with the help of COSY, TOCSY ROESY, and ^{1}H−^{13}C HMQC NMR experiments, along with the chemical shift data reported for the related NHC complexes.[45] For palladium complex **5a**, the ^{1}H NMR spectrum shows five distinct and well-defined resonances for allylic protons, typical of an ABCDX-type spin system. The strong σ-donor properties and greater *trans* influence of the carbene ligand compared with the chloride ligand causes the allylic carbon atom *trans* to carbene to be weakly bonded, consequently causing the asymmetry in the allylic bonding. The central allylic CH proton (H_2) appears as a complex multiplet at δ 4.68, whereas the allylic CH_2 protons pseudo-*trans* to carbene appear at δ 3.71 (dd, ^3J = 7.5 Hz, ^2J = 1.8 Hz, *syn* in relation to H_2) and δ 2.62 (d, ^3J = 13.8 Hz, *anti* in relation to H_2), and the CH_2 protons pseudo-*trans* to chloride resonate at δ 3.16 (d, ^3J = 6.7 Hz, *syn* in relation to H_2) and δ 1.71 (d, ^3J = 11.8 Hz, *anti* in relation to H_2), respectively. The ^{1}H NMR spectrum of **5a** also shows five resonances (δ 2.69 (3H), 2.66 (3H), 2.27 (6H), 1.53 (3H), and 1.38 (3H), respectively) for the mesityl CH_3 protons and a set of four broad resonances at δ 7.02, 7.01 6.79, and 6.82 for the mesityl *m*-CH protons, which suggests that the mesityl ring protons are in a slightly different chemical environment with a restricted rotation around the N−mesityl bonds on either side of the imidazole ring. The backbone protons (−NC*HCH*N−) resonate upfield at δ 6.09 (d, J = 9.3 Hz) and 6.07 for palladium complex **5a**, when compared with δ 6.61 observed for imidazolinium salt **3a**.

The ^{1}H NMR (room temperature, 291 K) of (η^3-C_3H_5)Pd(BIAN-SIPr)Cl, **5b**, shows the absence of one set of the characteristic resonances for isopropyl-CH_3, naphthyl-CH, and *m*-CH protons of the 2,6-diisopropylphenyl ring and a set of resonances for the allyl-CH_2 protons. The broad resonance observed for the backbone (−NC*HCH*N−), isopropyl-CH

(45) Filipuzzi, S.; Pregosin, P. S.; Albinati, A.; Rizzato, S. *Organometallics* **2008**, *27*, 437–444, and references therein..

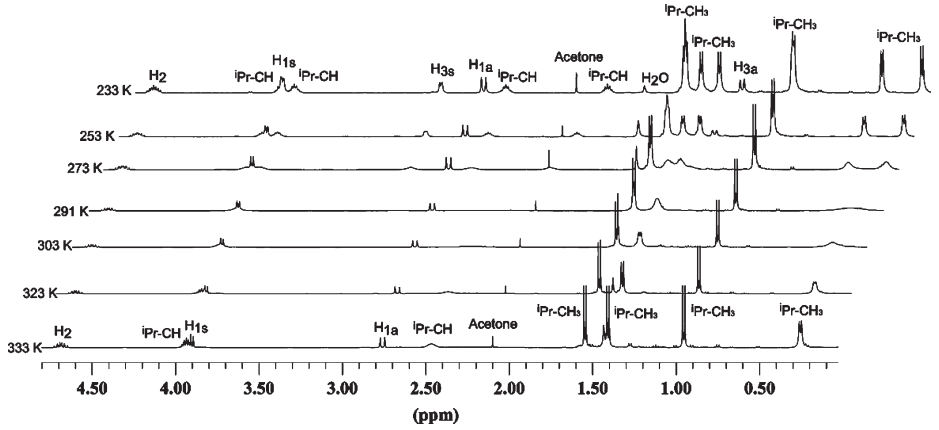

Figure 4. Selected ^{1}H VT-NMR spectra in the allylic region of (η^3-C_3H_5)Pd(BIAN-SIPr)Cl, **5b**.

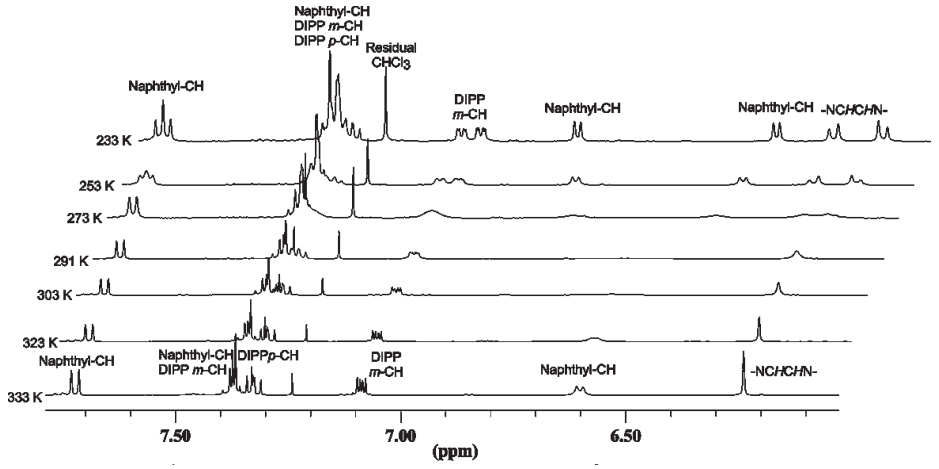

Figure 5. Selected ^{1}H VT-NMR spectra in the aromatic region of (η^3-C_3H_5)Pd(BIAN-H_2IPr)Cl, **5b**.

protons further suggests a dynamic fluxional behavior in the molecule. Complete freezing of the fluxional process was achieved at 233 K, and at this temperature assignment of the ^{1}H NMR data was made with the help of gCOSY, TOCSY, ROESY, and ^{1}H−^{13}C HMQC NMR spectroscopy. The ^{1}H VT-NMR spectrum in the high-field region is shown in Figure 4, and that in the aromatic region, in Figure 5. They further show the formation of only one diasteromer over a temperature range. The diisopropyl-CH_3 and methine (CH) protons resonate as a set of eight doublets, δ 1.50 (d, 3H, J = 6.2 Hz), 1.48 (d, 3H, J = 6.2 Hz), 1.40 (d, 3H, J = 6.8 Hz), 1.29 (d, 3H, J = 6.8 Hz), 0.86 (d, 3H, J = 6.7 Hz, ^{i}Pr-$C_{39}H_3$), 0.82 (d, 3H, J = 6.7 Hz), 0.30 (d, 3H, J = 6.7 Hz), and 0.08 (d, 3H, J = 6.7 Hz), and a set of four septets, δ 3.99−3.91 (m, 1H), 3.84 (sept, 1H, J = 6.6 Hz), 2.58 (sept, 1H, J = 6.7 Hz), and 1.97 (sept, 1H, J = 6.7 Hz), at 233 K, respectively, suggesting that all the diisopropyl methyl and diisopropyl methine protons are inequivalent. Upon warming the NMR sample, the resonances started to broaden and then coalesce to a set of four sharp doublets and a set of two broad septets at 333 K for the diisopropyl methyl and methine protons, respectively. At 233 K the resonance corresponding to the naphthyl-CH protons appears as a set of four doublets at δ 7.73 (d, 2H, J = 8.3 Hz), 7.72 (d, 2H, J = 8.3 Hz), 6.81 (d, ^3J = 6.8 Hz), and 6.36 (d, ^3J = 6.9 Hz) and a complex multiplet at δ 7.41−7.29, respectively, whereas a set of *m*-CH protons shows two doublets of doublets at δ 7.02 (dd, ^3J = 6.9 Hz, ^4J = 2.2 Hz) and 7.06 (dd, ^3J = 6.9 Hz, ^4J = 2.2 Hz), respectively. The backbone protons (−NC*H*C*H*N−) resonate upfield at δ 6.23 as a singlet from 291 to 333 K, whereas two doublets δ 6.13 (d, ^3J = 10 Hz) and 6.24 (d, ^3J = 6.8 Hz) were observed at 233 K. This reflects a high degree of asymmetry in the molecule at 333 K due to the hindered rotation around N−aromatic bond and the asymmetrically bonded allylic ligand (*vide infra*). The ^{1}H VT-NMR spectra also reveal that a set of resonances arising from the naphthyl-CH protons coalesce to one broad doublet δ 6.62 (d, ^3J = 6.8 Hz) at 333 K, suggesting a free rotation around the Pd−NHC bond. Similar behaviors were observed for the other set of naphthyl-CH, a set of *m*-CH for either side of the imidazole ring, and backbone (−NC*H*C*H*N−) protons. This dynamic behavior reflects the presence of a free rotation around the Pd−NHC bond.

The molecular structure of **5b**, Figure 10, shows that the mean plane passing through the imidazole ring is almost perpendicular (83.12°) to the plane that is composed of NHC-C, palladium, allylic C_{38}, C_{40}, and chloride ligands. Due to a bulky naphthyl group at the backbone (−NC*H*C*H*N−), a twist in the imidazole ring was also observed (*vide infra*), which in turn puts the aromatic rings on the either side of the imidazole ring in a slightly different environment. In principle, one should expect four nonequivalent diisopropyl groups and consequently four nonequivalent isopropyl methine protons. Whereas the observed peak pattern in the ^{1}H and ^{13}C NMR spectrum at 233 K suggests that all the diisopropyl methyl,

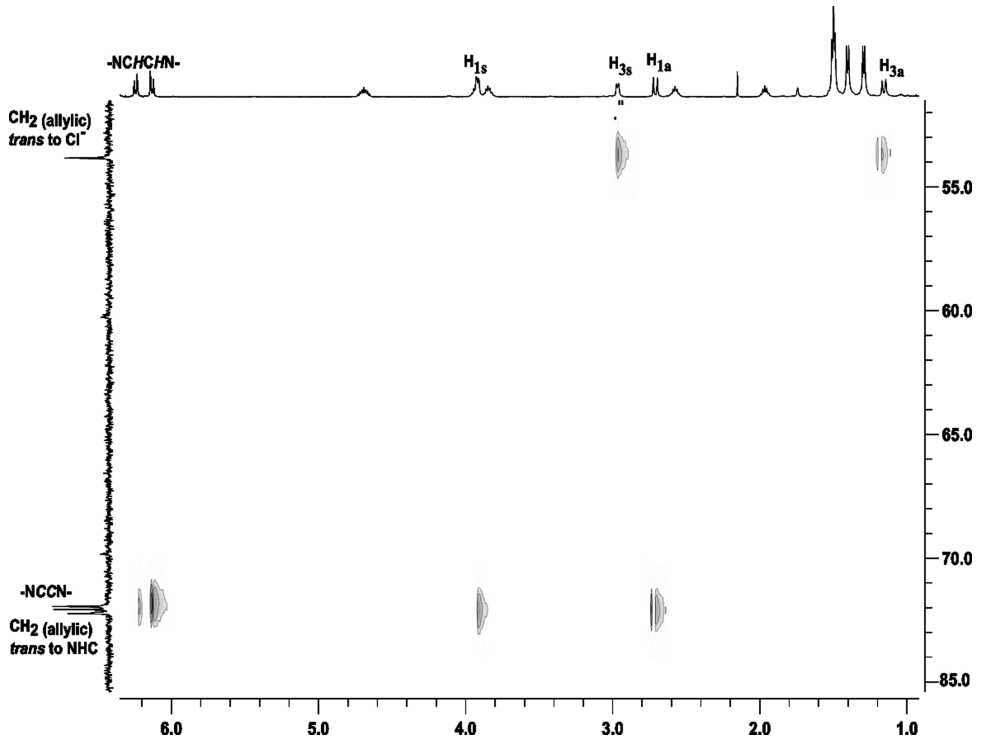

Figure 6. Slice of the $^1H-^{13}C$ HMQC (500 MHz, $CDCl_3$, 233 K) correlation for **5b**.

diisopropyl methine, and the N-aromatic ring protons/carbons are indeed nonequivalent due to restricted rotation around the N−diisopropylphenyl bonds on either side of the imidazole ring and asymmetrically bonded allyl ligand, consequently, all the naphthyl ring CH protons are also inequivalent (*vide supra*).

The $^1H-^1H$ ROESY NMR spectra, Figures 8 and 9, at 233 K, further show a selective exchange for the isopropyl methyl, and methine protons. Furthermore, the observed exchange cross process for the backbone (−NC*H*C*H*N−), naphthyl CH and the diisopropylphenyl *m*-CH protons on either side of the imidazole ring strongly confirms a free rotation around the Pd−NHC bond and a hindered rotation around the N−aromatic bond on either side of the imidazole ring; similar behaviors were also observed previously.[46,47]

A section of the ^1H VT-NMR spectrum in the allylic region, Figure 4, shows a typical ABCDX-type spin system for the allylic protons[45,48−50] at 233 K. Given the greater *trans* influence of the NHC group when compared with the chloride ligand, the positions of allylic CH_2 protons pseudo-*trans* to the NHC ligand were unambiguously assigned with the aid of $^1H-^{13}C$ HMBC and $^1H-^{13}C$ HMQC experiments. A section of the $^1H-^{13}C$ HMQC experiment is shown in Figure 6. The allylic CH_2 protons pseudo-*trans* to NHC appeared as a doublet at δ 3.92 (^3J = 7.2 Hz, H_{1s}, *syn* in relation to H_2) and 2.71 (^3J = 13.5 Hz, H_{1a}, *anti* in relation to H_2), while the corresponding protons pseudo-*trans* to chloride ligands appeared as doublets at δ 2.97 (^3J = 6.7 Hz, H_{3s}) and 1.15 (^3J = 12.2 Hz, H_{3a}) at 233 K, respectively. The chemical shift values observed for the allylic protons in (η^3-C_3H_5)Pd(BIAN-SIMes)Cl (**5a**) and (η^3-C_3H_5)Pd(BIAN-SIPr)Cl (**5b**) are consistent with the chemical shift values reported for related (η^3-C_3H_5)Pd(NHC)Cl complexes. Because of the strong σ-donor properties of NHC ligands, the selective opening of the allyl ligand *trans* to the NHC was expected exclusively on the grounds of the greater *trans* influence of the NHC ligand, when compared with the chloride ligand. As expected, upon warming the NMR sample, the allylic CH_2 (pseudo-*trans* to chloride) resonances started to broaden, and at 291 K they have completely disappeared into the baseline, whereas the resonances arising from the allylic CH_2 protons pseudo-*trans* to NHC remain sharp throughout. Complete coalescence for the allylic CH_2 pseudo-*trans* to chloride ligands was not observed due to the temperature limitation of the solvent. This kind of dynamic behavior is consistent with the selective $\eta^3-\eta^1$ opening of the allyl ligand under electronic control, followed by the rotation around the C−C bond, and then isomerization to $\eta^1-\eta^3$ to re-form the allyl ligand.-(Scheme 3). Such selective $\eta^3-\eta^1$ exchange processes are very well recognized for the chiral phosphine bidentate ligand systems due to their enhanced steric and electronic effects.[46,51−61]

(46) Filipuzzi, S.; Pregosin, P. S.; Albinati, A.; Rizzato, S. *Organometallics* **2008**, *27*, 437–444.
(47) Chernyshova, E. S.; Goddard, R.; Pörschke, K.-R. *Organometallics* **2007**, *26*, 3236–3251.
(48) Powell, J.; Shaw, B. L. *J. Chem. Soc. A* **1967**, *11*, 1839–1851.
(49) Ramey, K. C.; Statton, G. L. *J. Am. Chem. Soc.* **1966**, *88*, 4387–4389.
(50) Powell, J.; Robinson, S. D.; Shaw, B. L. *Chem. Commun.* **1965**, *5*, 78–79.
(51) Albinati, A.; Kunz, R.; Ammann, C. J.; Pregosin, P. S. *Organometallics* **1991**, *10*, 1800–1806.
(52) Gogoll, A.; Örnebro, J.; Grennberg, H.; Bäckvall, J.-E. *J. Am. Chem. Soc.* **1994**, *116*, 3631–3632.
(53) Herrmann, J.; Pregosin, P. S.; Salzmann, R.; Albinati, A. *Organometallics* **1995**, *14*, 3311–3318.
(54) Kumar, P. G. A.; Dotta, P.; Hermatschweiler, R.; Pregosin, P. S.; Albinati, A.; Rizzato, S. *Organometallics* **2005**, *24*, 1306–1314.
(55) Mikhael, I.; Goux-Henry, C.; Sinou, D. *Tetrahedron: Asymmetry* **2006**, *17*, 1853–1858.
(56) Pregosin, P. S.; Salzmann, R. *Coord. Chem. Rev.* **1996**, *155*, 35–68.
(57) Pregosin, P. S.; Salzmann, R.; Togni, A. *Organometallics* **1995**, *14*, 842–847.
(58) Statton, G. L.; Ramey, K. C. *J. Am. Chem. Soc.* **1966**, *88*, 1327–1328.
(59) Cesarotti, E.; Grassi, M.; Prati, L.; Demartin, F. *J. Organomet. Chem.* **1989**, *370*, 407–419.

Scheme 3. $\eta^3-\eta^1-\eta^3$ Isomerisation Process for Palladium Allyl Complex 5b

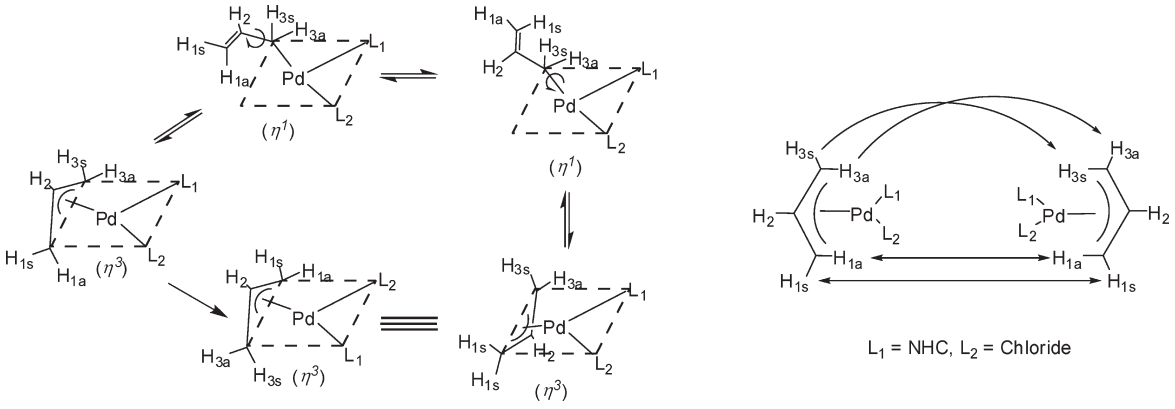

The π to σ equilibrium is well documented for Pd(η^3-C_3H_5)-(L_1)(L_2) complexes, where L_1 and L_2 = chloride, PPh_3, $P(OPh)_3$, DMSO, pyridine, and bidentate phosphine ligands. This is followed by temperature-dependent selective *syn* to *anti* interchange of the allylic protons, which usually takes place through the $\eta^3-\eta^1-\eta^3$ interconversion process under electronic or steric control[45,48−50,52−61] (Scheme 3).

The section of ROESY NMR (233 K) spectrum in the allylic region for palladium complex **5b** is given in Figure 8. To our surprise, the $^1H-^1H$ ROESY NMR spectrum shows selective exchange peaks only for the carbene ligand, whereas the peaks arising from the corresponding allyl interconversion process (*syn*→*anti and anti*→*syn*) for the protons *trans* to the chloride ligand (labeled H_3) are canceled out by a strong overlapping NOE peak. However, the only observed cross-peaks are the TOCSY breakthrough peak caused by *J*-coupling between the H_{1a}, H_{3s}, and H_{3a}, respectively. Furthermore, the dynamic NMR behavior observed over 233 to 333 K (Figure 4) for the allyl ligand and NHC ligand and the absence of the corresponding exchange cross-peaks in the $^1H-^1H$ ROESY NMR for the protons pseudo-*trans* to the NHC ligand (labeled H_1) strongly suggest the selective $\eta^3-\eta^1-\eta^3$ isomerization process is operative under electronic control. Therefore, after the selective $\eta^3-\eta^1-\eta^3$ isomerization process, the protons labeled H_1 (pseudo-*trans* to NHC) find themselves in the same environment, and this may be considered as *syn*→*syn* and *anti*→*anti* exchange processes. This is also further supported by the X-ray diffraction studies (*vide infra*), confirming that the allyl ligand is bound in the asymmetric fashion, with localized single and double bonds within the allyl ligand, Figure 7c.

In the $^{13}C\{^1H\}$ NMR spectrum the Pd−$C_{(carbene)}$ resonance is shifted to lower frequency at δ 210.6 (**5a**) and 213.4 (**5b**) when compared with imidazolin-2-ylidene δ 247.3 (**4a**) and 241.9 (**4b**);[39] this characteristic upfield shift is symptomatic of the coordination of saturated NHC with transfer of the electron density to the metal center and consistent with previously reported NHC palladium complexes.[45,62,63] Full ^1H and ^{13}C assignments are given in the Experimental Section.

X-ray Crystal Structure of (η^3-C_3H_5)Pd(BIAN-SIPr)Cl, 5b. Single crystals suitable for X-ray diffraction were grown by slow diffusion of pentane into a saturated dichloromethane solution. Two (alterable) ORTEP views of the molecule **5b** are shown in Figure 10, and the crystal data are summarized in Table 1 in the Supporting Information. The absolute configuration of the palladium complex **5b**, determined by X-ray analysis, reveals that the palladium has a distorted square-planar geometry, as expected for the palladium allyl complexes, but interestingly the Flack enantiopole parameter[64] gives a value of −0.06(3), suggesting the crystal consists of a single enantiomer despite the achiral nature of the complex. The geometry of the allyl ligand was interpreted with extreme caution in view of its disordered nature. It was also observed that the allyl group is bonded in an asymmetric mode; the $C_{38}-C_{39}$ and $C_{39}-C_{40}$ bond lengths are 1.321(8) and 1.549(9) Å, respectively, which indicates that the formal single and double bonds are partially localized. All attempts to enforce a symmetric geometry on the allyl ligand during refinement worsened the agreement with the X-ray data. Hydrogen atoms on the carbene ligand were positioned geometrically after each cycle, but it was not possible to locate the allyl hydrogen atoms unambiguously in the Fourier maps, as no appropriate prototype structure was available; therefore, they could not be positioned geometrically and are omitted from the model. They were, however, included in the calculation of the molecular formula, molecular weights, etc. The three-term Chebychev polynomial weighting scheme was then applied, and refinements converged satisfactory to give R = 0.0330 and R_w = 0.0327.

The carbene ligand is present in a plane normal to the plane of the molecule that comprises Pd, $C_{(carbene)}$, Cl, and two terminal carbon atoms of the allyl ligand. The Pd−$C_{(carbene)}$ and Pd−Cl bond lengths are 2.044(3) and 2.3715(3) Å, respectively, and consistent with the reported data for (η^3-C_3H_5)Pd(NHC)Cl complexes,[62,65] where NHC = SIMes, SIPr. The Pd−C_{38}, Pd−C_{39}, and Pd−C_{40} bond lengths are 2.204(6), 2.165(4), and 2.121(6) Å, respectively. Due to the large aromatic system at the C_2-C_3 bond, no large torsion angles for the palladium complex was expected, but to our surprise, upon coordination with palladium, a twist appears in the backbone, Figure 10, producing a torsion angle of 12.92°, which is approximately 10° greater than that observed for imidazolinium salt **3b**. In the molecular structure of

(60) Breutel, C.; Pregosin, P. S.; Salzmann, R.; Togni, A. *J. Am. Chem. Soc.* **1994**, *116*, 4067–4068.
(61) Wassenaar, J.; van Zutphen, S.; Mora, G.; Le Floch, P.; Siegler, M. A.; Spek, A. L.; Reek, J. N. H. *Organometallics* **2009**, *28*, 2724–2734.
(62) Jensen, D. R.; Sigman, M. S. *Org. Lett.* **2003**, *5*, 63–65.
(63) Viciu, M. S.; Germaneau, R. F.; Navarro-Fernandez, O.; Stevens, E. D.; Nolan, S. P. *Organometallics* **2002**, *21*, 5470–5472.
(64) Flack, H. D.; Bernardinelli, G. *J. Appl. Crystallogr.* **2000**, *33*, 1143.
(65) Viciu, M. S.; Navarro, O.; Germaneau, R. F.; Kelly, R. A., III; Sommer, W.; Marion, N.; Stevens, E. D.; Cavallo, L.; Nolan, S. P. *Organometallics* **2004**, *23*, 1629–1635.

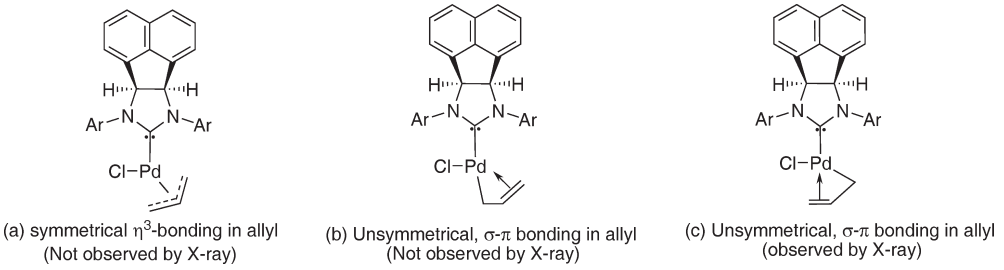

Figure 7. Allyl bonding mode for palladium complex **5b**.

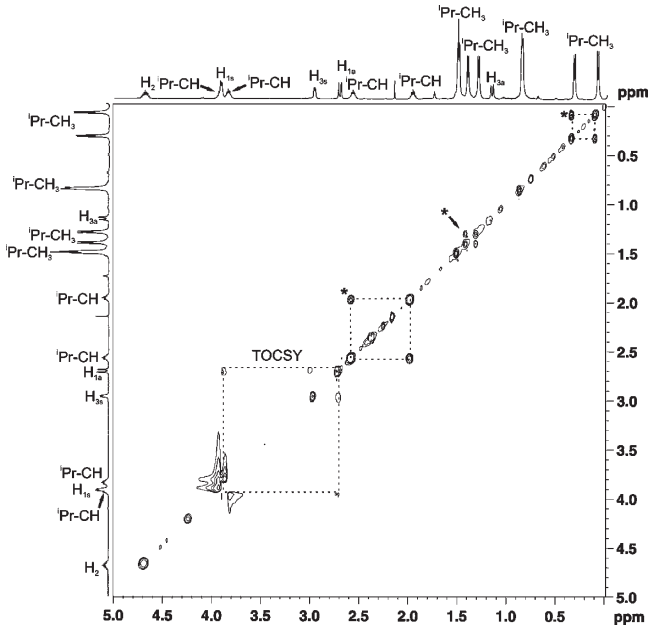

Figure 8. Section of the $^1H-^1H$ ROESY NMR (500 MHz, $CDCl_3$, 233 K) spectrum (negative phase) in the allylic region for **5b**, showing exchange (*) and the TOCSY cross-peaks.

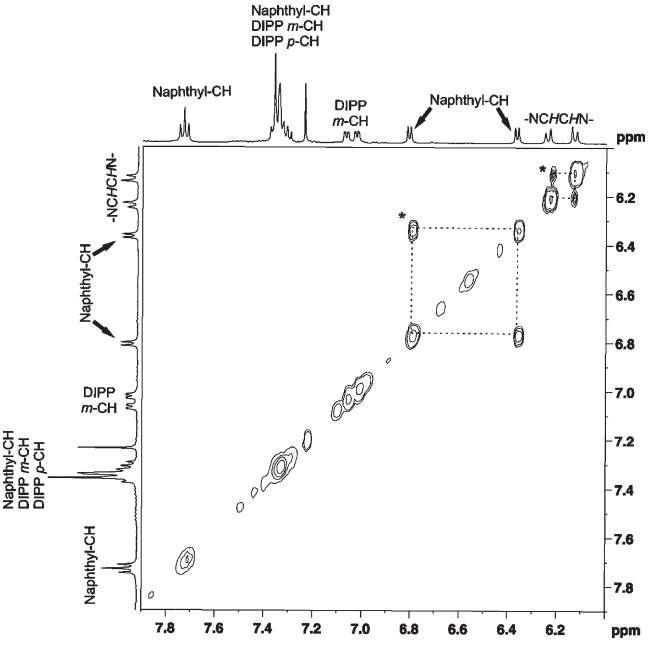

Figure 9. Section of the $^1H-^1H$ ROESY NMR (500 MHz, $CDCl_3$, 233 K) spectrum (negative phase) in the aromatic region for **5b**, showing exchange (*) cross-peaks.

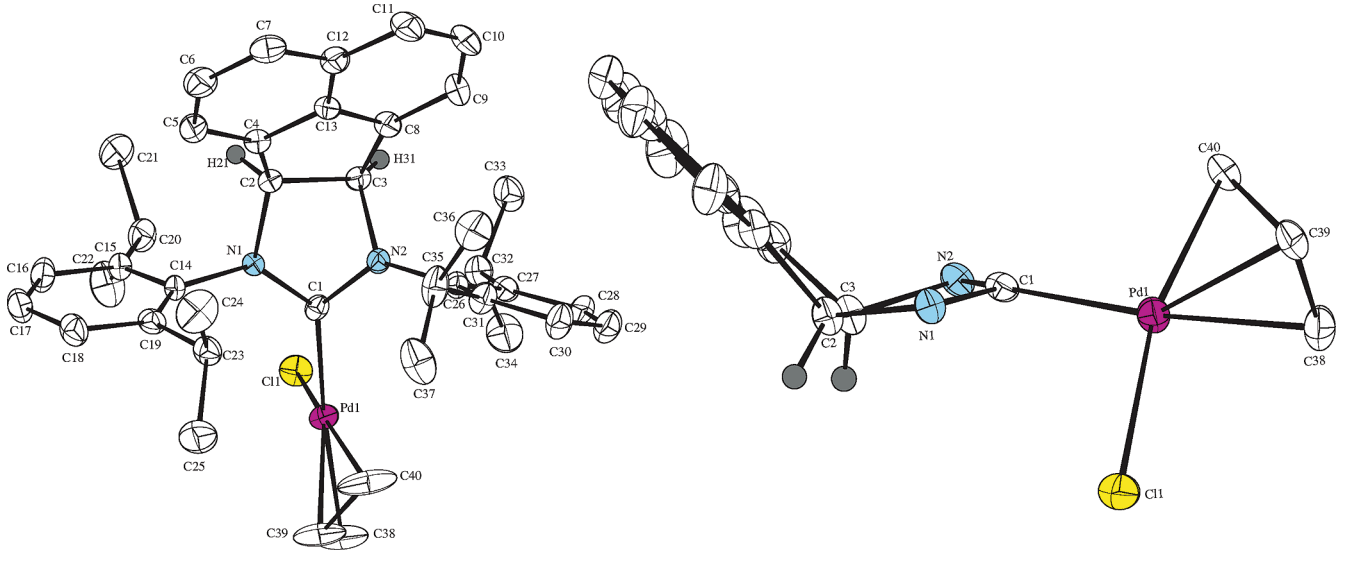

Figure 10. ORTEP diagram of the molecular structure of **5b** at 40% probability. Hydrogen atoms, minor orientation of the allyl group, and 2,6-diisopropylphenyl groups (structure on right) have been omitted for clarity.

imidazolinium salts the average $C_1-N_{1(2)}$ and $N_{1(2)}-C_{2(3)}$ bond lengths of 1.347 and 1.488 Å are slightly larger than the corresponding bond lengths observed for imidazolinium salt **3b**, which are indicative of the loss of electron density from the $C_1-N_{1(2)}$ bonds. The smaller $N_1-C_1-N_2$ bond angle of 108.4(2)° when compared with **3b** is also due to the loss of

Table 2. Comparison of Selected Bond Lengths(Å) and Angles (deg)

property	(η^3-C_3H_5)Pd-(BIAN-SIPr)Cl, **5b**	(η^3-C_3H_5)Pd-(SIPr)Cl[a]
	Bond Lengths	
Pd−$C_{(carbene)}$	2.044(3)	2.042(5)
Pd−Cl	2.3715(8)	2.376(14)
Pd−$C_{(trans\ to\ NHC)}$	2.204(6)	2.211(6)
Pd−C_{39}	2.165(4)	2.124(7)
Pd−$C_{(trans\ to\ chloride)}$	2.121(6)	2.098(6)
C_{38}−C_{39}	1.321(8)	1.304(1)
C_{39}−C_{40}	1.549(9)	1.407(9)
C_1−$N_{1(2)}$	1.344(3), 1.350(3)	1.344(7), 1.346(6)
$N_{1(2)}$−$C_{2(3)}$	1.484(3), 1.492(3)	1.489(7)
C_2−C_3	1.555(4)	1.516(9)
	Bond Angle (θ)	
N_1−C_1−N_2	108.4(2)	108.19(4)
	Torsion Angle (θ)	
N_1−C_2−C_3−N_2	12.9	19.8(6)

[a] Reference 65.

electron density from C_1−$N_{1(2)}$ bonds but of the same order as observed for the corresponding rhodium(I) and iridium(I) complexes.[39] The significantly larger N_1−C_2−C_4 and N_2−C_3−C_8 bond angles of 117.2(2)° and 116.2(3)° observed for **5b** are due to the greater interaction of bulky, more hindered isopropyl groups and further supported by the larger torsion angle of 12.9° when compared with 2.42° observed for **3b**. The angle between the best planes of the dihydroimidazole ring and the naphthyl group is 56.56°, whereas the angles between the best planes of the dihydroimidazole ring and the phenyl rings C_{15}−C_{14}−C_{19} and C_{31}−C_{26}−C_{27} are 65.19° and 82.28°, respectively. The angle between the mean plane passing through the imidazole ring and the plane composed of C_1−Cl_1−C_{38}−C_{40} is 83.15°. A comparison of the selected crystal data for **5b** with the related palladium complex (η^3-C_3H_5)Pd-(SIPr)Cl is given in Table 2. Complete details of the single-crystal X-ray analysis are given in the Supporting Information.

Catalytic Cross-Coupling Reactions. The Suzuki−Miyaura reaction,[66] the coupling of $ArB(OH)_2$ (Ar = phenyl or substituted aromatic groups) with aryl, vinyl, or alkyl halides, offers a mild, versatile, and dominant methodology for the construction of C−C bonds.[22] The popularity of the Suzuki−Miyaura reaction is due to the easy accessibility of a wide variety of air- and moisture-stable reactants that are nontoxic. In recent years, palladium N-heterocyclic carbene metal complexes have emerged as a new class of catalysts for cross-coupling reactions.[67−74] The catalytic cycle, Scheme 4, first involves the *in situ* reduction of Pd(II) complex to Pd(0)

Scheme 4. Catalytic Cycle for Suzuki−Miyaura and Buchwald−Hartwig Coupling Reactions

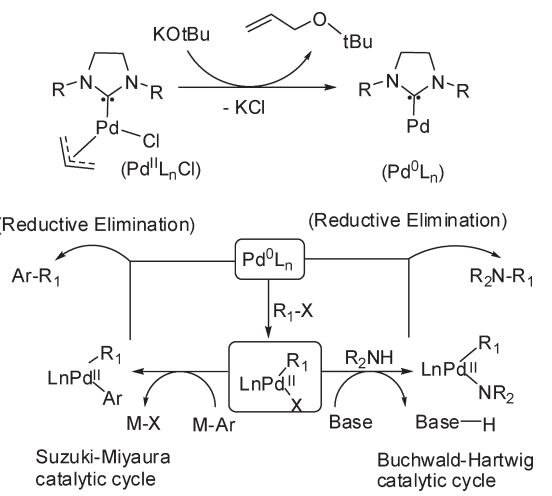

with the help of a suitable base, and then a monoligated Pd(0) species takes part in three discrete catalytic steps such as oxidative-addition, transmetalation, and then reductive-elimination to give the coupled product and regenerated Pd(0) species for the next catalytic cycle. The catalytic cycle suggests that a strong σ-donor ligand is needed for a facile oxidative addition, whereas a sterically bulky ligand is required for the reductive elimination step.[27,75,76] However, a recent mechanistic study by Fu et al. has shown that a bulky, sterically demanding ligand can have adverse effects on the oxidative-addition step;[72] therefore, for a highly active catalyst a delicate balance between the electronic and steric bulk is required.

The structure and electronic properties of the palladium complexes **5a** and **5b** appear to fulfill all the requirements for good catalysts in these cross-coupling reactions and proved to be thermally robust for C−C coupling reactions of activated and deactivated aryl halides with boronic acids, Table 3, and also for C−N bond formation with morpholine and *N*-methylaniline, Table 4. Our initial attempts using K_2CO_3 or Cs_2CO_3 failed to activate the catalyst. However, the Suzuki coupling reactions were then successfully performed using KO^tBu in 1,4-dioxane at 80 °C, unless otherwise stated. In some cases up to 5% homocoupling of the boronic acid substrate was observed as a side reaction (entries 2 and 5, Table 3). The optimum conversion of 90−96% was obtained for highly deactivated and hindered aryl bromides, 2,3,5,6-tetrafluorobromobenzene, and bromomesitylene (entries 4 and 5, Table 3). More than 99% conversions were obtained for hindered boronic acid using activated and deactivated aryl chlorides.

The first tin-free palladium-catalyzed carbon−nitrogen bond (aryl amination) formation was independently reported by Hartwig et al.[77,78] and Buchwald et al.[79,80] in

(66) Miyaura, N.; Suzuki, A. *Chem. Rev.* **1995**, *95*, 2457–2483.
(67) Altenhoff, G.; Goddard, R.; Lehmann, C. W.; Glorius, F. *J. Am. Chem. Soc.* **2004**, *126*, 15195–15201.
(68) Liu, J.; Robins, M. J. *Org. Lett.* **2004**, *6*, 3421–3423.
(69) Song, C.; Ma, Y.; Chai, Q.; Ma, C.; Jiang, W.; Andrus, M. B. *Tetrahedron* **2005**, *61*, 7438–7446.
(70) Hadei, N.; Kantchev, E. A. B.; O'Brien, C. J.; Organ, M. G. *Org. Lett.* **2005**, *7*, 1991–1994.
(71) Singh, R.; Viciu, M. S.; Kramareva, N.; Navarro, O.; Nolan, S. P. *Org. Lett.* **2005**, *7*, 1829–1832.
(72) Hills, I. D.; Netherton, M. R.; Fu, G. C. *Angew. Chem., Int. Ed.* **2003**, *42*, 5749–5752.
(73) Miura, M. *Angew. Chem., Int. Ed.* **2004**, *43*, 2201–2203.
(74) Wang, A.-E.; Zhong, J.; Xie, J.-H.; Li, K.; Zhou, Q.-L. *Adv. Syn. Catal.* **2004**, *346*, 595–598.
(75) Hadei, N.; Kantchev, E. A. B.; O'Brie, C. J.; Organ, M. G. *Org. Lett.* **2005**, *7*, 1991–1994.
(76) Christmann, U.; Vilar, R. *Angew. Chem., Int. Ed.* **2005**, *44*, 366–374.
(77) Louie, J.; Paul, F.; Hartwig, J. F. *Organometallics* **1996**, *15*, 2794–2805.
(78) Louie, J.; Hartwig, J. F. *Tetrahedron Lett.* **1995**, *36*, 3609–3612.
(79) Wolfe, J. P.; Wagaw, S.; Buchwald, S. L. *J. Am. Chem. Soc.* **1996**, *118*, 7215–7216.
(80) Guram, A. S.; Rennels, R. A.; Buchwald, S. L. *Angew. Chem., Int. Ed. Engl.* **1995**, *34*, 1348–1350.

Table 3. Palladium-Catalyzed Suzuki Coupling Reaction of Activated and Deactivated Aryl Halide[d]

Entry	Substrate	Product	Catalyst	Time (h)	GC Conv. (%)[a]
1	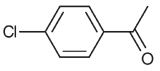	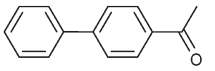	**5a**	1.2	98
			5b	1.0	95
2	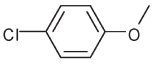	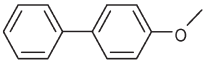	**5a**	0.8	96
			5b	1.0	95[b]
3	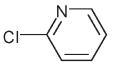	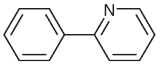	**5a**	1.0	98
4	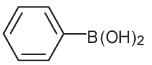 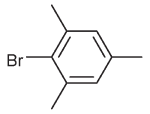	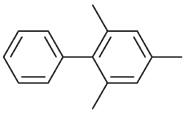	**5a**	1.0	70
				2.0	75
				12.0	90
5	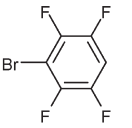	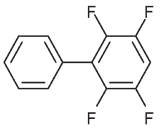	**5a**	3.5	96(85)[b,c]
6	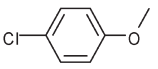	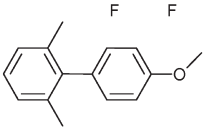	**5a**	1.0	≥ 99
7	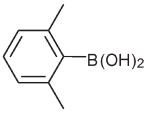 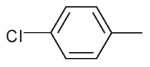	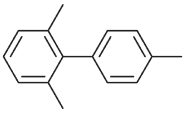	**5a**	1.0	≥ 99

[a] Average of two runs. [b] 5% biphenyl was observed. [c] Isolated yield in parentheses. [d] Standard conditions: 0.75 mmol of boronic acid, 0.5 mmol of aryl halide, 1.0 mmol of Cs_2CO_3, 1% Pd, 4.0 mL of dioxane, 80 °C.

Table 4. Palladium-Catalyzed Aryl Amination Reaction of Activated and Deactivated Aryl Halide[d]

Entry	Substrate	Product	Catalyst	Time (min)	GC Conv. (%)[a]
1	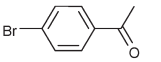	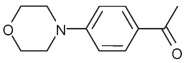	**5a**	90	≥ 99
			5b	120	97
2	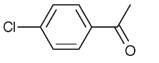	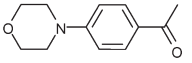	**5b**	120	80
				60	≥ 99[a]
3	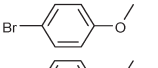	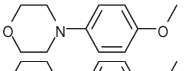	**5b**	10	98
4	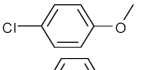	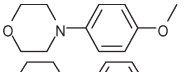	**5a**	45	≥ 99 (92)[b]
5	 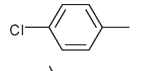	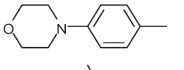	**5b**	75	≥ 99
6	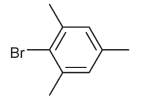	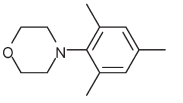	**5b**	90	65
				120	85(80)[b,c]
7	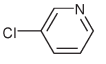	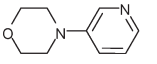	**5b**	90	≥ 99
8	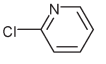	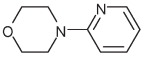	**5b**	180	85
9	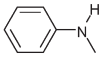 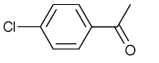	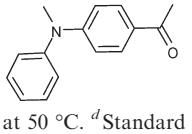	**5b**	90	94

[a] Average of two runs. [b] Isolated yields. [c] Reaction was carried out at 50 °C. [d] Standard conditions: 1.2 mmol of amine, 1.0 mmol of aryl halide, 1.5 mmol of KO^{t}Bu, 1% Pd, 4.0 mL of dioxane, room temperature.

1995, and thereafter Yamamoto et al.[81] and Hartwig et al.[21] have developed general methodologies for carbon−nitrogen bond formation reactions in small molecules. The catalytic cycle for palladium(II)-catalyzed aryl amination reactions also involves *in situ* formation of monoligated Pd(0) species. The representative catalytic cycle for the Suzuki and Buchwald−Hartwig coupling is shown in Scheme 4. The aryl amination reactions were performed using KO^{t}Bu in 1,4-dioxane at room temperature, except entry 2, Table 4, which was heated to 50 °C. The catalytic system using palladium complex **5b** can couple the deactivated aryl

(81) Yamamoto, T.; Nishiyama, M.; Koie, Y. *Tetrahedron Lett.* **1998**, *39*, 2367–2370.

bromide in less than 10 min (entry 3, Table 4), while hindered and deactivated bromomesitylene was coupled in 85% yield (entry 6, Table 4). Activated and deactivated aryl chlorides can be coupled in more than 95% yields at room temperature.

Conclusion

We have described a novel family of monodentate bulky backbone annulated imidazolinium ligand precursors and their corresponding palladium(II) carbene complexes. A bifurcated hydrogen bond between BF_4 anions and imidazolinium protons (−NC*H*N−) was observed for [(BIAN-SIMes)(H)]BF_4, **3a**. Furthermore the palladium complex (η^3-C_3H_5)Pd(BIAN-SIPr)Cl, **5b**, showed a selective temperature-dependent, electronically controlled $\eta^3-\eta^1-\eta^3$ exchange of the allyl ligand. The crystal structure of (η^3-C_3H_5)Pd(BIAN-SIPr)Cl, **5b**, represents a rare example in which a localized single and double bond within the allyl ligand was observed. The palladium(II) complexes show high activity in Suzuki-type C−C and Buchwald−Hartwig-type C−N cross-coupling reactions of activated and deactivated aryl halides.

Experimental Section

General Procedures. All manipulations were performed under dinitrogen using standard Schlenk vessel techniques or an inert atmosphere glovebox. All solvents were dried by passage through an alumina column under a positive pressure of dinitrogen and deoxygenated by bubbling dry dinitrogen through the dried solvents for 20 min before use. NMR spectra were recorded on either a Varian Unity Plus 500 (^{1}H at 500 MHz, ^{13}C at 125.7 MHz) or a Varian Mercury 300 (^{1}H at 300 MHz, ^{13}C at 75.5 MHz) spectrometer at room temperature unless otherwise stated. The spectra were referenced internally relative to the residual protio-solvent (^{1}H) and solvent (^{13}C) resonances, and chemical shifts were reported with respect to $\delta = 0$ for tetramethylsilane. Electrospray mass spectra were recorded in acetonitrile on a Micromass LC TOF spectrometer. Microanalyses were performed by the microanalytical laboratory of the Inorganic Chemistry Laboratory, University of Oxford. Gas chromatographs were recorded using a Perkin-Elmer XL 1100 instrument with a Perkin-Elmer NCI 900 Network Chromatography Interface using a fused silica, nonpolar SGE column 25QC2/BP1 1.0.

All reagents were purchased from Aldrich; metal precursors were from Johnson-Matthey and were used as received unless otherwise stated. The reagents BIAN-SIMes,[39] BIAN-SIPr,[39] and [Pd(η^3-C_3H_5)(μ-Cl)]$_2$[82] were prepared using published procedures. The base KO^{t}Bu was sublimed and kept in the inert atmosphere glovebox.

Synthesis of Bis[*N*,*N*′-(2,4,6-trimethylphenyl)imino]acenaphthene (1a). The compound bis[*N*,*N*′-(2,4,6-trimethylphenyl)imino]-acenaphthene was prepared using a modified method from that published by El-Ayaan et al.[40] Acenaphthenequinone (3.0 g, 16.5 mmol) was suspended in acetonitrile (100 mL) and heated under reflux (80 °C) for 60 min. Acetic acid (30 mL) was then added, and heating was continued until the acenaphthenequinone had completely dissolved. To this hot solution was added 2,4,6-trimethylaniline (4.8 g, 35.5 mmol) using a dropping funnel over the period of 20 min. The resulting solution was heated under reflux for another 3 h and cooled to room temperature. The precipitated orange-red solid was filtered, washed with pentane (3 × 10 mL), and dried in air. Yield: 6.5 g, 95%. The ^{1}H and ^{13}C NMR spectra were consistent with the reported data.[40]

Synthesis of Bis[*N*,*N*′-(2,6-diisopropylphenyl)imino]acenaphthene (1b). The compound bis[*N*,*N*′-(2,6-diisopropylphenyl)imino]-acenaphthene was prepared using a modified method from that published by Paulovicova et al.[41] Acenaphthenequinone (7.0 g, 38.4 mmol) was suspended in acetonitrile (150 mL) and heated under reflux (80 °C) for 60 min. Acetic acid (65 mL) was then added, and heating was continued until the acenaphthenequinone had completely dissolved. To this hot solution was added 2,6-diisopropylphenylaniline, 92% (16.0 g, 89.9 mmol), with the help of a dropping funnel over a period of 30 min, and the solution was heated under reflux for a further 5 h and then cooled to room temperature. The resulting orange-yellow solid was then filtered, washed with pentane (3 × 20 mL), and dried in air. Yield: 18.1 g, 94%. The ^{1}H and ^{13}C NMR spectra were consistent with the reported data.[41]

Synthesis of Bis[*N*,*N*′-(2,4,6-trimethylphenyl)amino]acenaphthene (2a). To a suspension of $LiAlH_4$ (0.23 g, 6.1 mmol) in diethyl ether (30 mL) was added dropwise a solution of bis[*N*,*N*′-(2,4,6-trimethylphenyl)imino]acenaphthene, **1a** (3.4 g, 8.1 mmol), in diethyl ether (40 mL) at 0 °C, and the mixture was stirred for 1 h. The reaction mixture was warmed to room temperature, stirred for an additional 3 h, and then quenched with 10% HCl solution in water. The product was extracted in CH_2Cl_2 (3 × 15 mL), dried, and purified by flash chromatography using CH_2Cl_2/pentane (70:30) to give an orange-yellow solid. Yield: 2.9 g, 85%. The ^{1}H and ^{13}C NMR spectra were consistent with the reported data.[43]

Synthesis of Bis[*N*,*N*′-(2,6-diisopropylphenyl)amino]acenaphthene (2b). To a suspension of $LiAlH_4$ (0.20 g, 5.3 mmol) in diethyl ether (60 mL) was dropwise added a diethyl ether (40 mL) solution of bis[*N*,*N*′-(2,6-diisopropylphenyl)imino]acenaphthene, **1b** (3.6 g, 7.19 mmol), at 0 °C, and the mixture was stirred for 1 h. The reaction mixture was warmed to room temperature and stirred for an additional 3 h and then quenched with a 10% HCl solution. The product was extracted in CH_2Cl_2 (3 × 15 mL), dried, and then purified by flash chromatography using CH_2Cl_2/pentane (70:30) to give an orange-yellow solid. Yield: 3.1 g, 86%. The ^{1}H and ^{13}C NMR spectra were consistent with the reported data.[83]

Synthesis of 7,9-Bis(2,4,6-trimethylphenyl)-6b,9a-dihydroacenaphtho[1,2-*d*]imidazolinium Tetrafluoroborate (3a). To a one-neck flask (250 mL) fitted with a fractional distillation column was added a solution of bis[*N*,*N*′-(2,4,6-trimethylphenyl)amino]-acenaphthene, **2a** (1.5 g, 3.5 mmol), in triethyl orthoformate (30 mL) and ammonium tetrafluoroborate (0.38 g, 3.5 mmol). The reaction mixture was heated at 135 °C with constant stirring for 3 h with the distillation of ethanol, during which time the color of the reaction mixture turned yellow-brown from the original yellow solution with the precipitation of an oily black solid. The reaction was cooled to room temperature, and the solid was separated by decanting the brown solution. The crude product was dissolved in CH_2Cl_2 (10 mL), filtered, and precipitated with diethyl ether (20 mL). The resulting brown solid was then filtered and washed with ice-cold diethyl ether/THF (40:60) (3 × 10 mL) to give an off-white solid, which was dried under vacuum. Yield: 1.1 g, 61%. Crystals suitable for diffraction study were grown by layering of pentane onto a saturated dichloromethane solution.

^{1}H NMR (300 MHz, 291.6 K, $CDCl_3$): δ 8.19 (s, 1H, −NC*H*N−), 7.89 (d, 2H, J = 8.2 Hz, naphthyl ring C*H*), 7.42 (t, 2H, J = 7.1 Hz, naphthyl ring C*H*), 7.08 (s, 2H, mesityl *m*-C*H*), 7.03 (d, 2H, J = 7.1 Hz, naphthyl ring C*H*), 6.87 (s, 2H, mesityl *m*-C*H*), 6.6 (s, 2H, −NC*H*C*H*N−), 2.60 (s, 6H, mesityl-C*H*$_3$), 2.34 (s, 6H, mesityl-C*H*$_3$), 1.42 (s, 6H, mesityl-C*H*$_3$). ^{13}C NMR (75.5 MHz, 293 K, $CDCl_3$): δ 157.1 (s, $C_{(-NCN-)}$), 128.8, 131.8, 135.6, 135.9, 136.1, 137.3, 140.8 (s, $C_{(\text{quaternary naphthyl and mesityl})}$), 130.1, 130.8 (s, *m*-$C_{(\text{mesityl})}$H), 122.3, 126.8, 128.7 (s, $C_{(\text{naphthyl})}$H), 70.6 (s, $C_{(-NCCN-)}$), 17.8, 18.3, 21.3 (s, *C*(mesityl)H$_3$). MS (ES$^+$, CH_3CN): m/z = 431.07 [M − BF_4]$^+$ (100%). Anal. Found (calcd): C 71.76 (71.82); H 5.98 (6.03); N 5.32 (5.40).

Synthesis of 7,9-Bis(2,6-diisopropylphenyl)-6b,9a-dihydroacenaphtho[1,2-*d*]imidazolinium Tetrafluoroborate (3b). To a one-neck flask (250 mL) fitted with a fractional distillation

(82) Tatsuno, Y.; Yoshida, T.; Otsuka, S. *Inorg. Syn.* **1990**, *28*, 343.

(83) Ishizaki, K.; Komuro, K.; Kato, H.; Suzuki, H. Production method of phenylsilane in the presence of diamine and transition metal catalyst. 2003277388, 20020325, **2003**.

column was added a solution of bis[*N*,*N*′-(2,6-diisopropylphenyl)amino]acenaphthene (**2b**) (3.9 g, 7.7 mmol) in triethyl orthoformate (60 mL) and ammonium tetrafluoroborate (0.81 g, 7.7 mmol). The reaction mixture was heated at 135 °C with constant stirring for 3 h with the distillation of ethanol, during which time the color of the reaction mixture turned brown from the original yellow solution with the precipitation of an oily black solid. The reaction was cooled to room temperature, and the solid was separated by decanting the brown solution. The crude product was dissolved in CH_2Cl_2 (10 mL), filtered, and precipitated with diethyl ether (20 mL). The resulting brown solid was then filtered and washed with ice-cold diethyl ether/THF (40:60) (3 × 20 mL) to give an off-white solid, which was dried under vacuum. Yield: 3.4 g, 74%. Crystals suitable for diffraction study were grown by layering of pentane onto a saturated dichloromethane solution.

^{1}H NMR (500 MHz, 293 K, $CDCl_3$): δ 8.18 (s, 1H, −NC*H*N−), 7.89 (d, 2H, J = 8.3 Hz, naphthyl ring C*H*), 7.53 (t, 2H, J = 7.8 Hz, naphthyl C*H*), 7.48 (d, 2H, J = 7.4 Hz, *p*-CH), 7.45 (dd, 2H, J = 7.4 Hz, J = 1.4 Hz, *m*-CH), 7.23 (dd, 2H, J = 7.6 Hz, J = 1.4 Hz, *m*-CH), 6.92 (d, 2H, J = 7.1 Hz, naphthyl ring CH), 6.67 (s, 2H, −NC*H*C*H*N−), 3.43 (sept, 2H, J = 6.8 Hz, ^{i}Pr-CH), 1.94 (sept, 2H, J = 6.6 Hz, ^{i}Pr-CH), 1.55 (d, 6H, J = 6.6 Hz, ^{i}Pr-CH_3), 1.34 (d, 6H, J = 6.6 Hz, ^{i}Pr-CH_3), 0.89 (d, 6H, J = 6.7 Hz, ^{i}Pr-CH_3), 0.72 (d, 6H, J = 6.6 Hz, ^{i}Pr-CH_3). ^{13}C{^{1}H} NMR (125.7 MHz, 293 K, $CDCl_3$): 156.3 (s, $C_{(-NCN-)}$), 127.8, 131.9, 135.5, 136.9, 146.5, 147.2 (s, $C_{(\text{quaternary naphthyl and 2,6-diisopropylphenyl})}$), 131.7 (s, *p*-*C*H), 128.5, 127.1, (s, $C_{(\text{naphthyl})}$H), 125.7, 124.7 (s, *m*-*C*H), 122.8 (s, $C_{(\text{naphthyl})}$H), 72.9 (s, $C_{(-NCCN-)}$), 29.5, 29.0 (s, $C_{(\text{iPr})}$H), 26.7, 25.1, 23.9, 22.3 (s, $C_{(\text{iPr})}H_3$). MS (ES$^+$, CH_3CN): m/z = 515.43 [M − BF_4]$^+$ (100%). Anal. Found (calcd): C 72.91 (73.75); H 7.20 (7.19); N 4.69 (4.65).

Synthesis of (η^3-Allyl)Pd(BIAN-SIMes)Cl (5a). To a stirred solution of [Pd(η^3-C_3H_5)(μ-Cl)]$_2$ (0.2 g, 0.55 mmol) in THF (5.0 mL) at −78 °C was added dropwise a solution of BIAN-SIMes (**4a**) (0.49 g, 1.14 mmol) in THF (5.0 mL). The reaction mixture was stirred for 10 min and then gradually warmed to room temperature and stirred for an additional 3 h. The mixture was then filtered, and the pale yellow solution was evaporated to reduce the total volume to 2 mL. Addition of pentane (10 mL) gave an orange-yellow solid, which was filtered, washed with ice-cold diethyl ether/pentane (20:80) (5 mL) and pentane (2 × 5 mL), and dried under vacuum. Yield: 0.49 g, 73%.

^{1}H NMR (500 MHz, 293 K, $CDCl_3$): δ 7.81 (d, 1H, J = 8.2 Hz, naphthyl ring CH), 7.80 (d, 1H, J = 8.1 Hz, naphthyl ring CH), 7.43 (dt, 2H, J = 8.3 Hz, J = 1.7 Hz, naphthyl ring C*H*), 7.04 (s, 1H, mesityl *m*-C*H*), 7.03 (s, 1H, mesityl *m*-C*H*), 6.89 (d, 1H, J = 7.2 Hz, naphthyl ring C*H*), 6.85 (d, 1H, J = 7.2 Hz, naphthyl ring C*H*), 6.83 (s, 1H, mesityl *m*-C*H*), 6.81 (s, 1H, mesityl *m*-C*H*), 6.10 (d, 1H, J = 9.3 Hz, −NC*H*C*H*N−), 6.09 (d, 1H, J = 9.2 Hz, −NC*H*C*H*N−), 4.76−4.66 (m, 1H, allyl H), 3.74 (dd, 1H, J = 7.5 Hz, J = 1.8 Hz, allyl $C_{(\text{pseudo-}trans\text{ to NHC})}H_s$), 3.18 (d, 1H, J = 6.9 Hz, allyl $C_{(\text{pseudo-}trans\text{ to Cl})}H_s$), 2.71 (s, 3H, mesityl-$CH_3$), 2.67 (s, 3H, mesityl-$CH_3$), 2.65 (d, 1H, J = 13.4 Hz, allyl allyl $C_{(\text{pseudo-}trans\text{ to NHC})}H_a$), 2.30 (s, 6H, mesityl-$CH_3$), 1.73 (d, 1H, J = 12.0 Hz, allyl$_{(\text{pseudo-}trans\text{ to Cl})}H_a$), 1.60 (s, 3H, mesityl-$CH_3$), 1.40 (s, 3H, mesityl-$CH_3$). ^{13}C{^{1}H} NMR (75.5 MHz, 293 K, CD_2Cl_2): δ 210.6 (s, $C_{(\text{Pd-carbene})}$), 139.9,139.2, 138.2, 138.0, 137.7, 137.1, 136.8, 136.7, 136.4, 134.6, 131.6, (s, $C_{(\text{quaternary naphthyl})}$ and $C_{(\text{quaternary mesityl})}$), 128.3, 129.2, 129.3, 129.6 (s, $C_{(\text{mesityl})}$H), 121.5, 121.8, 125.4, 125.5, 128.0 (s, $C_{(\text{naphtyl})}$H), 114.5 (s, allyl CH), 71.6 (s, allyl $C_{(trans\text{ to Carbene})}H_2$), 71.1 (s, $C_{(-NCHCHN-)}$), 51.5 (s, allyl $C_{(trans\text{ to chloride})}H_2$), 20.9 (s, $C_{(\text{mesityl})}H_3$), 18.7, 18.9, 19.0 (br s, $C_{(\text{mesityl})}H_3$). MS (ES$^+$, CHCN): m/z = 618.43 [M − Cl + CH_3CN]$^+$ (100%), 577.21 [M − Cl]$^+$ (50%). Anal. Found (calcd): C 66.39 (66.56); H 5.81 (5.75); N 4.43 (4.57).

Synthesis of (η^3-Allyl)Pd(BIAN-SIPr)Cl (5b). To a stirred solution of [Pd(η^3-C_3H_5)(μ-Cl)]$_2$ (0.3 g, 0.82 mmol) in THF (10 mL) at −78 °C was added dropwise a solution of BIAN-SIPr (**4b**) (0.88 g, 1.72 mmol) in THF (5.0 mL). The reaction mixture was stirred for 10 min, gradually warmed to room temperature, and stirred for 3 h. The reaction mixture was filtered, and the pale yellow solution was evaporated to reduce the total volume to 2 mL. Addition of pentane (10 mL) gave the product as an off-white solid. This was washed with pentane (3 × 5 mL) and dried under vacuum. Yield: 0.87 g, 76%.

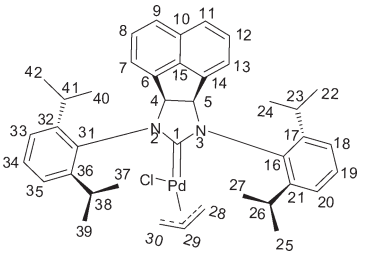

^{1}H NMR (500 MHz, 233 K, $CDCl_3$): δ 7.73 (d, 2H, J = 8.3 Hz, naphthyl $C_{11}H$), 7.73 (d, 2H, J = 8.3 Hz, naphthyl C_9H), 7.41−7.29 (m, 6H, *p*-$C_{19}H$, *m*-$C_{18}H$, *m*-$C_{33}H$, *p*-$C_{34}H$, naphthyl C_8H, naphthyl $C_{12}H$), 7.08 (dd, 1H, J = 6.9 Hz, J = 2.2 Hz, *m*-$C_{35}H$), 7.02 (dd, 1H, J = 6.9 Hz, J = 2.2 Hz, *m*-$C_{19}H$), 6.81 (d, 1H, J = 6.81 Hz, naphthyl-$C_{13}H$), 6.36 (d, 1H, J = 6.9 Hz, naphthyl-C_7H), 6.24 (d, 1H, J = 10.0 Hz, −NC_4HCHN−), 6.13 (d, 1H, J = 10.0 Hz, −NCHC_5HN−), 4.75−4.57 (m, 1H, allyl $C_{29}H$), 3.99−3.91 (m, 2H, ^{i}Pr-C_{23}H, allyl $C_{30}H_s$), 3.84 (sept, 1H, J = 6.6 Hz, ^{i}Pr-$C_{41}H$), 2.97 (d, 1H, J = 6.7 Hz, allyl $C_{28}H_s$), 2.71 (d, 1H, J = 13.5 Hz, allyl $C_{30}H_a$), 2.58 (sept, 1H, J = 6.7 Hz, ^{i}Pr-$C_{38}H$), 1.97 (sept, 1H, J = 6.7 Hz, ^{i}Pr-C_{26}H), 1.50 (d, 3H, J = 6.2 Hz, ^{i}Pr-$C_{24}H_3$), 1.48 (d, 3H, J = 6.2 Hz, ^{i}Pr-$C_{42}H_3$), 1.40 (d, 3H, J = 6.8 Hz, ^{i}Pr-$C_{22}H_3$), 1.29 (d, 3H, J = 6.8 Hz, ^{i}Pr-$C_{40}H_3$), 1.15 (d, 1H, J = 12.2 Hz, allyl $C_{28}H_a$), 0.86 (d, 3H, J = 6.7 Hz, ^{i}Pr-$C_{39}H_3$), 0.82 (d, 3H, J = 6.7 Hz, ^{i}Pr-$C_{27}H_3$), 0.30 (d, 3H, J = 6.7 Hz, ^{i}Pr-$C_{37}H_3$), 0.08 (d, 3H, J = 6.7 Hz, ^{i}Pr-$C_{25}H_3$). ^{13}C{^{1}H} NMR (125.7 MHz, 233 K, $CDCl_3$): δ 213.4 (s, C_1), 148.5 (s, C_{17}), 147.9 (s, C_{21}), 146.7 (s, C_{36}), 146.4 (s, C_{32}), 138.4 (s, C_6), 137.5 (s, C_{14}), 136.9 (s, C_{15}), 134.5 (s, C_{31}), 134.4 (s, C_{17}), 131.1(s, C_{10}), 128.9 (s, C_{19}), 128.4 (s, C_{34}), 128.1 (s, C_{12}), 127.9 (s, C_8), 125.9 (s, C_{11}), 125.5 (s, C_9), 125.3 (s, C_{33}), 124.6 (s, C_{18}), 124.3 (s, C_{35}) 124.0 (s, C_{20}), 122.3 (s, C_{13}), 122.2 (s, C_7), 114.6 (s, C_{29}), 72.2 (s, C_{30}),72.1 (s, C_4) 71.9 (s, C_5), 53.8 (s, C_{28}), 29.2 (s, C_{41}), 28.7 (s, C_{23}), 28.2 (s, C_{26}), 27.9 (s, C_{38}), 26.8 (s, C_{22}), 25.9 (s, C_{40}), 24.9 (s, C_{39}), 24.9 (s, C_{27}), 24.5 (s, C_{24}), 24.4 (s, C_{42}), 24.1 (s, C_{25}), 23.9 (s, C_{37}). MS (ES$^+$, CHCN): m/z = 661.48 [M − Cl]$^+$ (100%). Anal. Found (calcd): C 69.01 (68.86); H 6.68 (6.76); N 3.93 (4.02).

Catalytic Studies. Typical Suzuki Coupling Procedure. A small Schlenk vessel was charged with aryl halide (0.5 mmol), boronic acid (0.75 mmol), KO^{t}Bu (1.0 mmol), and 4.0 mL of 1,4-dioxane in a glovebox. The catalyst (1.0 mol %) solution in 1,4-dioxane (0.25 mL) was added through the Suba seal, and the mixture was stirred at room temperature for 5 min. The catalytic mixture was then stirred at 80 °C for the indicated period of time (Table 3). The GC was calibrated with the authenticated samples of the coupled product, and the progress of the reaction was monitored by GC. The GC conversions were optimized in each case and reported as an average of two GC runs. For isolation of the products, the contents of the Schlenk vessel were mixed with silica gel and evaporated. The product/silica gel mixture was placed on the top of the flash chromatography column and eluted with a mixture of pentane and diethyl ether (90:10) (Table 3, entry 5). The product was analyzed by NMR, and the data were compared with the literature.[84]

Typical C−N Coupling Procedures. A small Schlenk vessel was charged with aryl halide (1.0 mmol), amine (1.2 mmol), KO^{t}Bu (1.5 mmol), and 4.0 mL of 1,4-dioxane in a glovebox. The catalyst (1.0 mol %) solution in 1,4-dioxane was added through the Suba

(84) Wei, Y.; Kan, J.; Wang, M.; Su, W.; Hong, M. *Org. Lett.* **2009**, *11*, 3346–3349.

seal, and the mixture was stirred for the indicated period of time at room temperature, unless otherwise stated (Table 4). The gas chromatograph was calibrated with the authenticated samples of the coupled product, and the progress of the reaction was monitored by GC. The GC conversions were optimized in each case and reported as an average of two GC runs. For isolation of the products, the contents of the Schlenk vessel were quenched with an aqueous solution of NH_4Cl and extracted in CH_2Cl_2. The organic fractions were mixed with silica gel and evaporated. The product/silica gel mixture was placed on the top of the flash chromatography column, and the product was purified by flash chromatography. The isolated products were analyzed by NMR, and the data were compared with the literature values.[85]

Acknowledgment. We thank the Royal Society for a University Research Fellowship (K.S.C.) and the Ministry of Science and Technology (MOST) and Lady Margaret Hall, University of Oxford, for graduate funding (S.D.). Special thanks to Dr. Nick Rees, Inorganic Chemistry Laboratory, Department of Chemistry, University of Oxford, for his help in the NMR studies and useful discussions, and Dr. David J. Watkin for helpful discussions on crystallography. S.D. thanks Dr. Howard Hunter, Department of Chemistry, York University, Toronto, Canada, for his help in reprocessing the NMR data.

Supporting Information Available: Crystallographic data (CIF) and a table containing a summary of crystal data are available free of charge via the Internet at http://pubs.acs.org. The structures reported in this paper have been deposited with the Cambridge Crystallographic Data Centre with CCDC reference numbers 714509 (**3a**), 714510 (**3b**), and 714511 (**5b**).

(85) Viciu, M. S.; Kissling, R. M.; Stevens, E. D.; Nolan, S. P. *Org. Lett.* **2002**, *4*, 2229–2231.